

# A Predictive Length-Dependent Saturation Current Model Based on Accurate Threshold Voltage Modeling

Khée Yong Lim<sup>\*</sup>, Xing Zhou<sup>\*</sup> and David Lim<sup>†</sup>

<sup>\*</sup> School of Electrical and Electronic Engineering, Nanyang Technological University,  
Nanyang Avenue, Singapore 639798, exzhou@ntu.edu.sg

<sup>†</sup> Chartered Semiconductor Manufacturing Ltd.  
60 Woodlands Industrial Park D, Street 2, Singapore 738406

## ABSTRACT

This paper presents a compact length-dependent saturation current ( $I_{dsat}$ ) model for deep-submicron MOSFET's based on accurate modeling of the threshold voltage ( $V_{th}$ ). The proposed unified model has considered all the important two-dimensional (2-D) short-channel effects, such as  $V_{th}$  roll-up and roll-off, drain-induced barrier lowering (DIBL), transverse-field mobility degradation and series resistance. The unique feature of the compact model is its ability to correlate to process variations such as implantation dose and energy. The model is verified with measured  $I_{dsat}$  data for various bias conditions and process split-run.

**Keywords:** Saturation current, threshold voltage, short-channel effect, compact modeling, process correlation.

## INTRODUCTION

The turn-on current of a MOSFET is one of the most important device parameters for advanced digital circuits as it determines the delay of logic gates. For a fixed-dimension MOSFET, its turn-on current, also known as saturation current ( $I_{dsat}$ ), is normally defined as the drain current at gate ( $V_{gs}$ ) and drain ( $V_{ds}$ ) biases both being equal to its power supply ( $V_{dd}$ ). It is well known from semiconductor theory that MOSFET's  $I_{dsat}$  is related to its device dimension, gate oxide thickness, high-field mobility, source and drain series resistance, gate- and substrate-bias conditions, and most importantly, its bias-dependent threshold voltage ( $V_{th}$ ). In this paper, an improved bias-dependent  $V_{th}$  model [1] that relates to process conditions is proposed and discussed, thereby, a predictive  $I_{dsat}$  model, which also correlates to process conditions, is presented. The proposed saturation current model is compared and verified with experimental data of a 0.25- $\mu\text{m}$  2.5-volt CMOS technology.

## MODEL

The theoretical threshold voltage of a MOSFET consists of three components, namely, the flat-band voltage ( $V_{FB}$ ),

the channel surface potential ( $\phi_s$ ), and the potential across the gate insulator ( $V_{ox}$ ), which can be expressed as:

$$V_{th} = V_{FB} + \phi_s + \frac{Q_B}{C_{ox}}$$

However, this simple model is only valid for long-channel devices because it does not account for 2-D effects, such as charge sharing, lateral doping pile-up and DIBL. A predictive bias-dependent  $V_{th}$  model that accounts for the above effects has been developed [1], [2]. An extension of that model is used in this work, which consists of only five important process-dependent parameters and two auxiliary DIBL parameters, namely,  $N_s$ ,  $\lambda$ ,  $\alpha$ ,  $\beta$ ,  $\kappa$  and  $i$ ,  $j$ , respectively. The improved  $V_{th}$  model is as follows:

$$V_{th} = V_{FB} + \phi_s + \gamma \sqrt{\phi_{s0} - V_{bs}} \left[ 1 - \frac{\lambda \zeta}{L_{eff}} \left( \sqrt{\phi_s - V_{bs}} + \frac{jV_{ds}}{\sqrt{\phi_s - V_{bs}}} \right) \right]$$

$$\zeta = \sqrt{\frac{2\epsilon_{si}}{qN_{eff}}}$$

$$\phi_{s0} = \frac{2kT}{q} \ln \left( \frac{N_{eff}}{n_i} \right)$$

$$\phi_s = \phi_{s0} - \Delta\phi_s$$

$$\Delta\phi_s = \frac{1}{\cosh \left( \frac{L_{eff}}{2l_\alpha} \right)} \left[ (V_{bi} - \phi_{s0}) \cosh \left( \frac{z}{2} \right) + \frac{iV_{ds}}{2} \frac{\sinh \left( \frac{L_{eff}}{2l_\alpha} - \frac{z}{2} \right)}{\sinh \left( \frac{L_{eff}}{2l_\alpha} \right)} \right]$$

$$N_{eff} = N_s + \frac{\kappa N_s}{\cosh(L_{eff}/2l_\beta)}$$

$$l_\alpha = \alpha (\phi_{s0} - V_{bs})^{0.25}$$

$$l_\beta = \beta (\phi_{s0} - V_{bs})^{0.25}$$

$$z = \ln \left( \frac{V_{bi} - \phi_{s0} + V_{ds}}{V_{bi} - \phi_{s0}} \right)$$

Each of the seven empirical fitting parameters has their own physical representation that characterizes the individual short-channel effects. The first parameter  $N_s$

represents the effective vertical nonuniform channel doping profile, which shifts the  $V_{th}$ - $L_g$  curve in parallel. All the other parameters affect the threshold voltage in short-channel regime only. The parameters  $\kappa$  and  $\beta$  characterize the reverse short channel effect ( $V_{th}$  roll-up).  $\kappa$  determines the degree of  $V_{th}$  roll-up while  $\beta$  sets the onset of  $V_{th}$  roll-up. Similarly, the normal short-channel effect ( $V_{th}$  roll-off) is modeled by the two parameters  $\lambda$  and  $\alpha$ .  $\lambda$  is introduced to model charge sharing whereas  $\alpha$  is for surface-potential lowering based on the quasi 2-D formulation [3]. The new auxiliary parameters  $i$  and  $j$  are introduced in this work to fine tune the DIBL dependency, which are used to model the asymmetric nature of the source and drain depletion region at high  $V_{ds}$  condition.

Once an accurate  $V_{th}$  model is available, developing an  $I_{dsat}$  model is mainly a matter of mobility and series-resistance modeling. The  $I_{dsat}$  model in [4] is employed, combined with our  $V_{th}$  model to predict experimental  $I_{dsat}$ - $L_g$  data measured from the same wafer split-lots. The  $I_{dsat}$  model considers all the important short-channel effects, which include perpendicular-field mobility degradation, velocity saturation, as well as source/drain series resistance. The saturation current model is expressed as follows:

$$I_{dsat} = I_{dsat0} \left( 1 - \frac{2I_{dsat0}R_s}{V_{gs} - V_{th}} + \frac{I_{dsat0}R_s}{V_{gs} - V_{th} + E_{sat}L_{eff}} \right)$$

$$I_{dsat0} = v_{sat} C_{ox} \frac{(V_{gs} - V_{th})^2}{V_{gs} - V_{th} + E_{sat}L_{eff}}$$

$$E_{sat} = \frac{2v_{sat}}{\mu_{eff}}$$

$$\mu_{eff} = \frac{\mu_0}{1 + \left( \frac{V_{gs} + V_{th}}{5.4t_{ox}} \right)^{1.85}}$$

In the above saturation current expression, the parameter  $\mu_0$  represents the low-field mobility. It is used as a technology-dependent fitting parameter. On the other hand,  $\mu_{eff}$  is the effective mobility including the effect of perpendicular-field degradation. The values of the saturation velocity  $v_{sat}$  are fixed at  $8 \times 10^6$  and  $6 \times 10^6$  cm/s for electron and hole, respectively [5]. The  $I_{dsat0}$  expression represents the saturation current without taking into account of the series-resistance effect. However, for short-channel devices, due to the increased drive current, the potential drop across the source and drain series resistance cannot be neglected. The above  $I_{dsat}$  expression is used to model the series-resistance effect.

## EXPERIMENTAL VERIFICATION

An empirically-based model will not be useful unless a consistent and simple parameter-extraction procedure can be adopted, nor will it be of any interest if experimental

data are needed to extract the parameters every time the model is used. The compact  $V_{th}$  model employs a simple, five-step, parameter-extraction procedure, which requires the measured  $V_{th}$ - $L_g$  data from the same process with only five sets of measurements:  $V_{th}(\text{long } L_g)$  for all  $V_{bs}$ ,  $V_{th}(\text{low } V_{ds}, \text{high } V_{bs})$ ,  $V_{th}(\text{low } V_{ds}, \text{low } V_{bs})$ ,  $V_{th}(\text{high } V_{ds}, \text{low } V_{bs})$  and  $V_{th}(\text{high } V_{ds}, \text{high } V_{bs})$  for all  $L_g$ .

A simple nonlinear regression on the theoretical long-channel threshold voltage expression, fitting the long-channel  $V_{th}$ - $V_{bs}$  data is used to extract  $N_s$ . The improved  $V_{th}$  model for short-channel devices can also be used since the values of ( $\lambda$ ,  $\alpha$ ,  $\beta$ ,  $\kappa$ ,  $i$ ,  $j$ ) will not affect the long-channel  $V_{th}$ . The extracted  $N_s$  value will be fixed in the subsequent steps. Nonlinear regression on the improved  $V_{th}$  equation is then performed by fitting the  $V_{th}(\text{low } V_{ds}, \text{high and low } V_{bs})$  vs.  $L_g$  data to extract  $\lambda$ ,  $\alpha$ ,  $\beta$ , and  $\kappa$ . To characterize the DIBL effect, additional parameters  $i$  and  $j$  are needed. With fixed  $\lambda$ ,  $\alpha$ ,  $\beta$  and  $\kappa$  extracted at low  $V_{ds}$ ,  $i$  and  $j$  are extracted by fitting the  $V_{th}(\text{high } V_{ds}, \text{low and high } V_{bs})$  vs.  $L_g$  data at high  $V_{ds}$ .

With additional long-channel  $V_{th}(V_{bs})$  data for different wafer-splits, the parameter  $N_s$  in the  $V_{th}$  model can correlate to process variables such as  $V_{th}$ -adjustment implant dose ( $\Phi$ ) and punchthrough implant energy ( $E$ ).

Once the  $V_{th}$  model is completely characterized, (by  $N_s$ ,  $\lambda$ ,  $\alpha$ ,  $\beta$ ,  $\kappa$ ,  $i$ ,  $j$ ), the low-field mobility ( $\mu_0$ ) and series resistance ( $R_s$ ) are extracted by fitting to only one set of  $I_{dsat}$ - $L_g$  data at  $V_{ds} = V_{gs} = V_{dd}$ . Then, a complete compact  $I_{dsat}$  model with drawn gate length ( $L_g$ ), bias voltages ( $V_{gs}$ ,  $V_{ds}$ ,  $V_{bs}$ ) and process variables (implant dose  $\Phi$  and energy  $E$ ) as input parameters is available.

The excellent prediction of the  $I_{dsat}$  model to the experimental data has been demonstrated in Figs. 1–4. The empirical correlation between the channel doping parameter ( $N_s$ ) and the implant dose and energy, which is extracted from long-channel  $V_{th}$  data (shown in the insets of Figs. 3 and 4), applies equally well to the saturation current.

Figures 1 and 2 show the model (*lines*) as compared to the measured data (*symbols*) for different gate and substrate biases, respectively. The  $V_{th}$  model parameters are extracted at  $V_{ds} = 0.1/2.5$  V and  $V_{bs} = 0/-2.7$  V. Excellent prediction of  $I_{dsat}$  at the intermediate biases  $V_{gs} = V_{ds} = 1$  V and  $V_{bs} = -0.9/-1.8$  V demonstrates the accuracy of the model. Figures 3 and 4 illustrate the predictability of the model (*lines*) as compared to the experimental data (*symbols*) for different  $V_{th}$ -adjustment implant dose ( $\Phi$ ) and punchthrough implant energy ( $E$ ), respectively. The parallel shift in the measured  $I_{dsat}$  has been well predicted by the shift in  $V_{th}$  due to the change in the substrate doping profile (long- and short-channel devices), which is related to the implant dose  $\Phi$  and energy  $E$  through linear empirical correlation, as shown in the insets of Figs. 3 and 4. Once the correct channel-length dependent  $V_{th}$  parameters ( $N_s$ ,  $\lambda$ ,  $\alpha$ ,  $\beta$ ,  $\kappa$ ,  $i$ ,  $j$ ) and  $I_{dsat}$  parameters ( $\mu_0$ ,  $R_s$ ) are determined, the same set of parameters can be applied to various process and bias conditions.

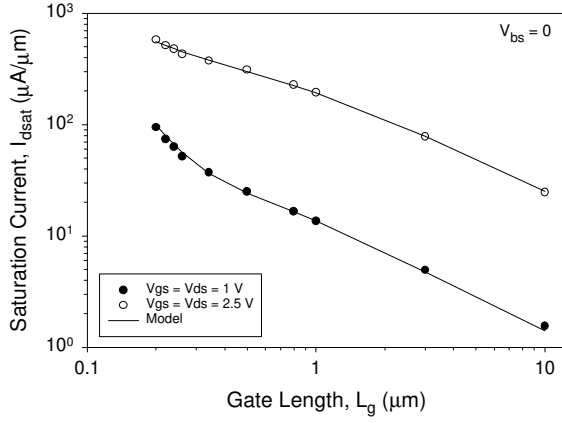


Figure 1: Measured (*symbols*) and modeled (*lines*) saturation current vs. gate length for different supply voltage  $V_{dd}$  (with  $V_{gs} = V_{ds} = V_{dd}$ ). Only the  $V_{dd} = 2.5$  V data are used for  $\mu_0$  and  $R_s$  extraction. All others are predictions by the model.

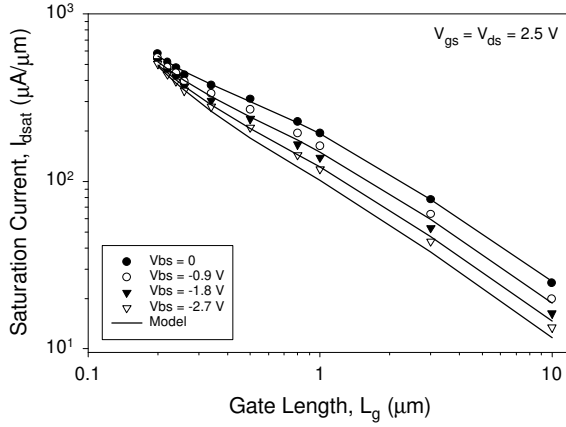


Figure 2: Measured (*symbols*) and modeled (*lines*) saturation current vs. gate length for different substrate bias  $V_{bs}$ . The  $V_{bs}$  dependency is modeled by the parameters in the  $V_{th}$  model.

The essence of the proposed compact-modeling approach is to predict physical behavior by interpolation. This means that one needs to design the experiment to cover a wide range of interest (e.g., full range of  $L_g$ ,  $V_{bs}$ , and  $V_{ds}$ ) such that process-dependent empirical parameters can be extracted at the “extreme” conditions. Thereby, the model can be employed for prediction by interpolation at intermediate values of the variables without performing nonlinear regression on every set of experimental data.

## CONCLUSION

The proposed model discussed in this work is simple and accurate, which is attributed to the accurate and physical modeling of the short-channel threshold voltage.

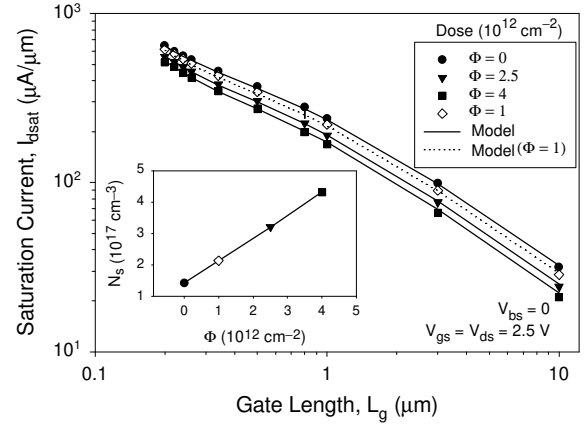


Figure 3: Measured (*symbols*) and modeled (*lines*) saturation current vs. gate length for different  $V_{th}$ -adjustment implant dose  $\Phi$ . The inset shows the extracted linear correlation between  $N_s$  and  $\Phi$  extracted from the  $V_{th}$  model.

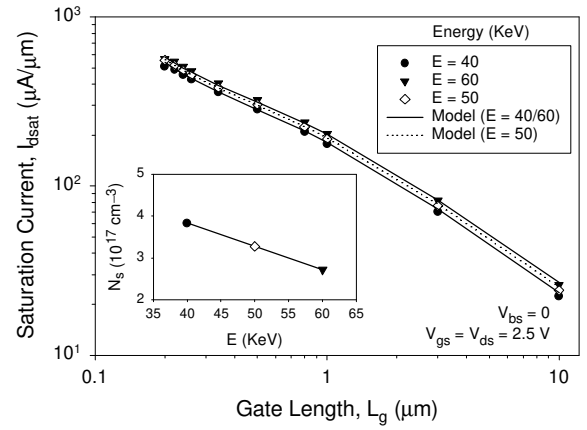


Figure 4: Measured (*symbols*) and modeled (*lines*) saturation current vs. gate length for different punchthrough implant energy  $E$ . The inset shows the extracted linear correlation between  $N_s$  and  $E$  extracted from the  $V_{th}$  model.

With minimum effort in model parameter extraction and correlation to process conditions, the model can predict the length-dependent saturation current at all bias conditions. This work has demonstrated an efficient and accurate approach to modeling deep-submicron MOSFET's, which is very useful for reducing experimental wafer split-lot and for process control and optimization.

## REFERENCES

- [1] X. Zhou, K. Y. Lim, and D. Lim “A General Approach to Compact Threshold Voltage Formulation Based on 2-D Numerical Simulation and Experimental Correlation for Deep-Submicron ULSI Technology

Development,” submitted to *IEEE Trans. Electron Devices*.

- [2] K. Y. Lim, X. Zhou, D. Lim, Y. Zu, H. M. Ho, K. Loiko, C. K. Lau, M. S. Tse, and S. C. Choo, “A Predictive Semi-Analytical Threshold Voltage Model for Deep-Submicron MOSFET’s,” *Proc. 1998 Hong Kong Electron Devices Meeting*, Aug. 1998, pp. 114–117.
- [3] Z.-H. Liu, C. Hu, J.-H. Huang, T.-Y. Chan, M.-C. Jeng, P. K. Ko, and Y. C. Cheng, “Threshold Voltage Model for Deep-Submicrometer MOSFET’s,” *IEEE Trans. Electron Devices*, vol. 40, no. 1, pp. 86–94, 1993.
- [4] K. Chen, H. C. Wann, J. Duster, D. Pramanik, S. Naraini, P. K. Ko and C. Hu, “An accurate semi-empirical saturation drain current model for LDD N-MOSFET,” *IEEE Electron Device Lett.*, vol. 17, no. 3, pp. 145–147, 1996.
- [5] *VLSI Electronics: Microstructure Science—Advanced MOS Device Physics*, edited by N. G. Einspruch, Academic Press, New York, vol. 18, p. 18, 1988.